

Table S1: Breast Pre-cancer Atlas Retrospective RAHBT Cohort for LCM. Related to Figure 1 and Table 1.

| | RAHBT | | | | | |
|------------------------------|---------------------------------|--|--|-------------------------------------|---|---------------------|
| | DCIS without recurrence (N=184) | DCIS with Ipsilateral DCIS Recurrence (N=17) | DCIS with Ipsilateral Invasive Recurrence (N=29) | DCIS with Contralateral DCIS (N=19) | DCIS with Contralateral Invasive Disease (N=16) | RAHBT Total (N=265) |
| Year of Diagnosis | | | | | | |
| Median | 2002 | 2005 | 2000 | 2002 | 1991 | 2002 |
| Age at Diagnosis | | | | | | |
| Median | 53 | 57 | 48 | 57 | 54 | 53 |
| Mean (±SD) | 55.6 (±11.4) | 61.1 (±12.8) | 49.9 (±10.3) | 55.9 (±9.9) | 58.2 (±12.2) | 55.5 (±11.5) |
| Grade | | | | | | |
| 1 | 51 [27.7%] | 3 [17.6%] | 8 [27.6%] | 7 [36.8%] | 4 [25.0%] | 73 [27.5%] |
| 2 | 65 [35.3%] | 7 [41.2%] | 15 [51.7%] | 8 [42.1%] | 7 [43.8%] | 102 [38.5%] |
| 3 | 65 [35.3%] | 6 [35.3%] | 4 [13.8%] | 4 [21.1%] | 5 [31.3%] | 84 [31.7%] |
| Missing | 2 [1.1%] | 1 [5.9%] | 2 [6.9%] | 0 | 0 | 6 [2.3%] |
| Pathologic Tumor Size | | | | | | |
| Median | NA | NA | NA | NA | NA | NA |
| Mean (±SD) | NA | NA | NA | NA | NA | NA |
| Marker Status | | | | | | |
| ER(+) | 123 [66.8%] | 11 [64.7%] | 24 [82.8%] | 17 [89.5%] | 14 [87.5%] | 189 [71.3%] |
| ER(-) | 61 [33.2%] | 6 [35.3%] | 5 [17.2%] | 2 [10.5%] | 2 [12.5%] | 76 [28.7%] |
| | | | | | | |
| ER(+) Dx before 2000 | 46 [25.0%] | 2 [11.8%] | 10 [34.5%] | 7 [36.8%] | 9 [56.2%] | 74 [27.9%] |
| ER(+) Dx 2000 & after | 77 [41.8%] | 9 [52.9%] | 14 [48.3%] | 10 [52.6%] | 5 [31.2%] | 67 [25.3%] |
| ER(-) Dx before 2000 | 29 [15.8%] | 3 [17.6%] | 4 [13.8%] | 2 [10.5%] | 1 [6.3%] | 87 [32.8%] |
| ER(-) Dx 2000 & after | 32 [17.4%] | 3 [17.6%] | 1 [3.4%] | 0 | 1 [6.3%] | 37 [14.0%] |
| Treatment | | | | | | |
| Lumpectomy w Radiation | 91 [49.5%] | 12 [70.6%] | 18 [62.1%] | 8 [42.1%] | 9 [50.0%] | 17 [51.7%] |
| Lumpectomy no Radiation | 34 [18.5%] | 5 [29.4%] | 7 [24.1%] | 1 [5.3%] | 0 | 47 [17.7%] |
| Lumpectomy Radiation Unknown | 3 [1.6%] | 0 | 1 [3.4%] | 1 [5.3%] | 1 [6.3%] | 6 [2.3%] |
| Mastectomy | 56 [30.4%] | 0 | 3 [10.3%] | 9 [47.4%] | 7 [43.8%] | 75 [28.3%] |

| | | | | | | |
|---|------------------------|--------------------|--------------------|---------------------|--------------------|--------------------|
| Time to Recurrence* (months) | | | | | | |
| Median | 111* | 49 | 80 | 81 | 56 | 62.3 |
| Mean (\pm SD) | 127.1 (\pm 84.4) | 61.5 (\pm 43.6) | 93.2 (\pm 74.2) | 107.3 (\pm 89.1) | 71.3 (\pm 56.3) | 85.5 (\pm 70.6) |
| Margins | | | | | | |
| Ink on tumor | 9 [4.9%] | 2 [11.8%] | 2 [6.9%] | 3 [15.8%] | 2 [12.5%] | 17 [6.4%] |
| <2mm | 24 [13.0%] | 3 [17.6%] | 3 [10.3%] | 3 [15.8%] | 3 [18.8%] | 36 [13.6%] |
| At least 2mm | 27 [14.7%] | 4 [23.5%] | 2 [6.9%] | 1 [5.3%] | 1 [6.3%] | 38 [14.3%] |
| Clear, unknown mm | 81 [44.0%] | 8 [47.1%] | 17 [58.6%] | 10 [52.6%] | 4 [25.0%] | 118 [44.5%] |
| Missing | 43 [23.4%] | 0 | 5 [17.2%] | 2 [10.5%] | 6 [37.5%] | 56 [21.1%] |
| Race | | | | | | |
| White | 138 [75.0%] | 12 [70.6%] | 22 [75.9%] | 15 [78.9%] | 10 [62.5%] | 197 [74.3%] |
| Black | 45 [24.5%] | 5 [29.4%] | 7 [24.1%] | 3 [15.8%] | 6 [37.5%] | 66 [24.9%] |
| Asian | 0 | 0 | 0 | 0 | 0 | 0 |
| Pacific Islander | 0 | 0 | 0 | 1 [5.3%] | 0 | 1 [0.4%] |
| Other | 0 | 0 | 0 | 0 | 0 | 0 |
| Unknown | 1 [0.5%] | 0 | 0 | 0 | 0 | 1 [0.4%] |

*To end of follow-up for no recurrence

Table S2: Breast Pre-cancer Atlas Multi-scale Characterization Assays. Related to Figure 1.

| Assay | Scale | Type of Data | Integration and validation with other assays | Analyzed in RAHBT | Analyzed in RAHBT LCM | Analyzed in TBCRC |
|---|----------------------------|---|--|---|-----------------------------------|---|
| RNA-seq (Single duct, tumor microenvironment) | Duct, organ, normal tissue | Whole transcriptome gene expression profiling per single duct | Gene expression and prediction of cell type composition (CibersortX) confirmed by MIBI (single cell) | Figure 2B, C, E, G Figure 3 Figure 5F | Figure 4B, C Figure 6A-C, E, G | Figure 2A, D, F Figure 3, Figure 4A, C Figure 5F |
| Low-pass whole genome DNA-seq | Duct and adjacent normal | CNV profiling per single duct | Analysis of CNV supported by RNA-seq (single duct) and MIBI (single cell) | Figure 5A-E | NA | Figure 5A-E |
| Multiplex IHC (MIBI) | Cell | 1. Cell type 2. Proteomic analysis | Analysis of protein expression and cell type supported by RNA-seq of ducts (CibersortX) | NA | Figure 4D, E, F Figure 6D, F | NA |

Figure S1

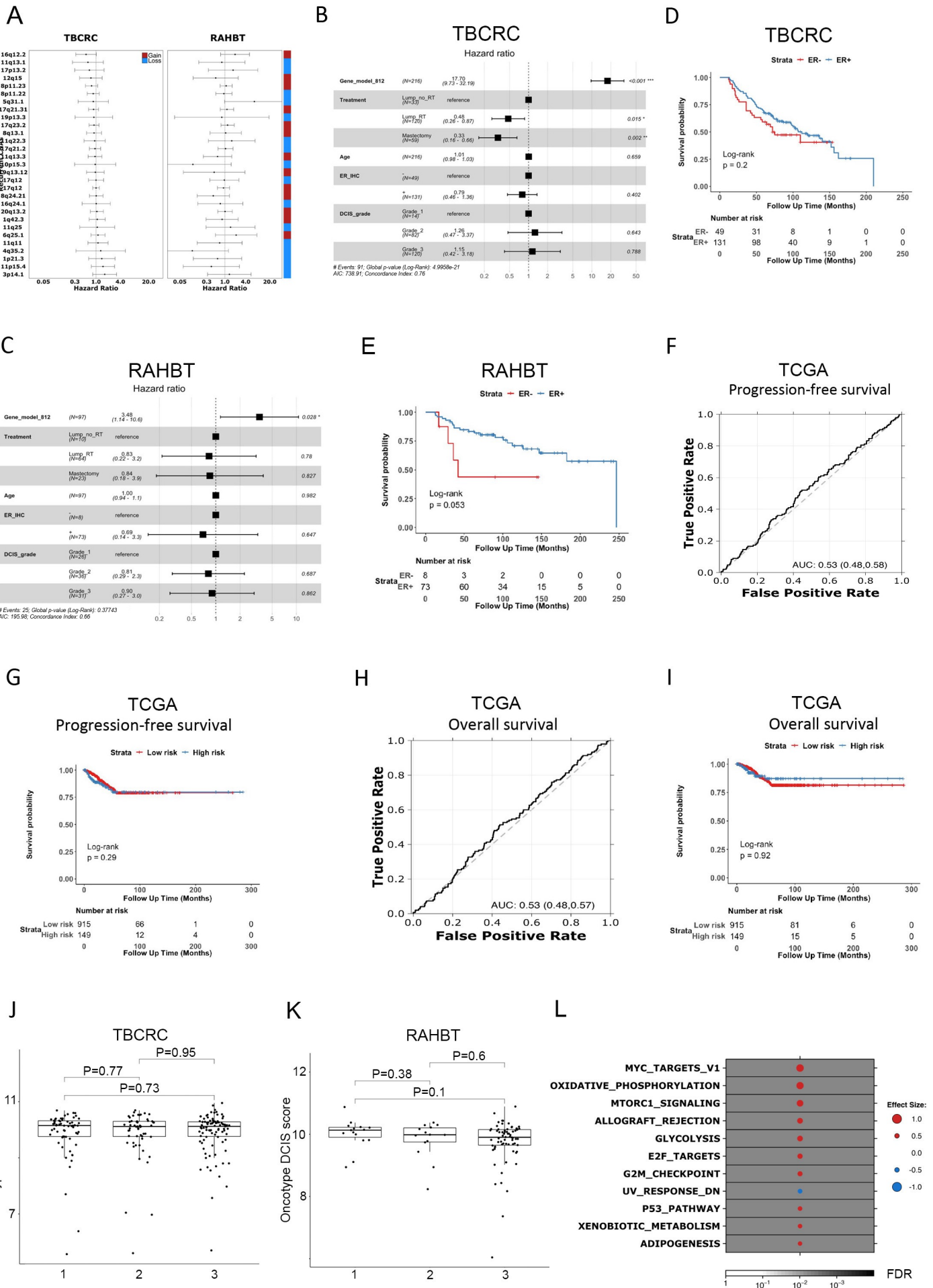


Figure S1: Outcome analysis. Related to Figure 2.

A) Forest plot showing hazard ratios from CoxPH modeling of the 29 recurrent copy number aberrations (CNAs) association with progression. Vertical dotted line represent hazard ratio = 1. The covariate on the right indicates if the CNA is a gain (red) or loss (blue). **B-C)** Forest plot of multivariable Cox regression analysis including 812 gene classifier (high- vs. low-risk groups), treatment, age, DCIS grade, and ER status by IHC for any iBE with full follow-up in TBCRC (**B**) and RAHBT (**C**). **D-E)** Kaplan-Meier plot of time to progression (any iBE, full follow-up) stratified by clinical ER status in TBCRC (**D**) and RAHBT (**E**). P-values from log-rank tests. **F)** ROC curve of the 812 gene classifier tested towards progression-free survival in TCGA IBC samples. **G)** Kaplan-Meier plot of time to progression in TCGA IBC samples. P-value from log-rank test. **H)** ROC curve of the 812 gene classifier tested towards overall survival in TCGA IBC samples. **I)** Kaplan-Meier plot of time to death in TCGA IBC samples. P-value from log-rank test. **J-K)** Box plot of Oncotype DX DCIS score in the three different outcome groups in TBCRC (**J**) and RAHBT (**K**). 1: DCIS with DCIS recurrence. 2: DCIS with IBC recurrence. 3: DCIS with no recurrence. The score was calculated as described by Solin *et al*¹⁸ but based on RNA-seq raw reads instead of Ct values from RT-qPCR. P-values from Wilcoxon rank sum test. Boxplots represent median, 0.25 and 0.75 quantiles with whiskers at 1.5x interquartile range. **L)** Gene Set Enrichment Analysis (GSEA) with Hallmark gene sets of the differentially expressed genes between cases with any iBE at 5 years after treatment vs the rest in TBCRC. Only significant pathways shown (FDR<0.05). Pathways sorted by effect size. Size of the dot and color represents the magnitude and direction of pathway deregulation, *i.e.*, blue indicates the pathway is downregulated while red indicates the pathway is upregulated. Background shading indicates false discovery rate (FDR). Effect size and FDR from GSEA algorithm.

Figure S2

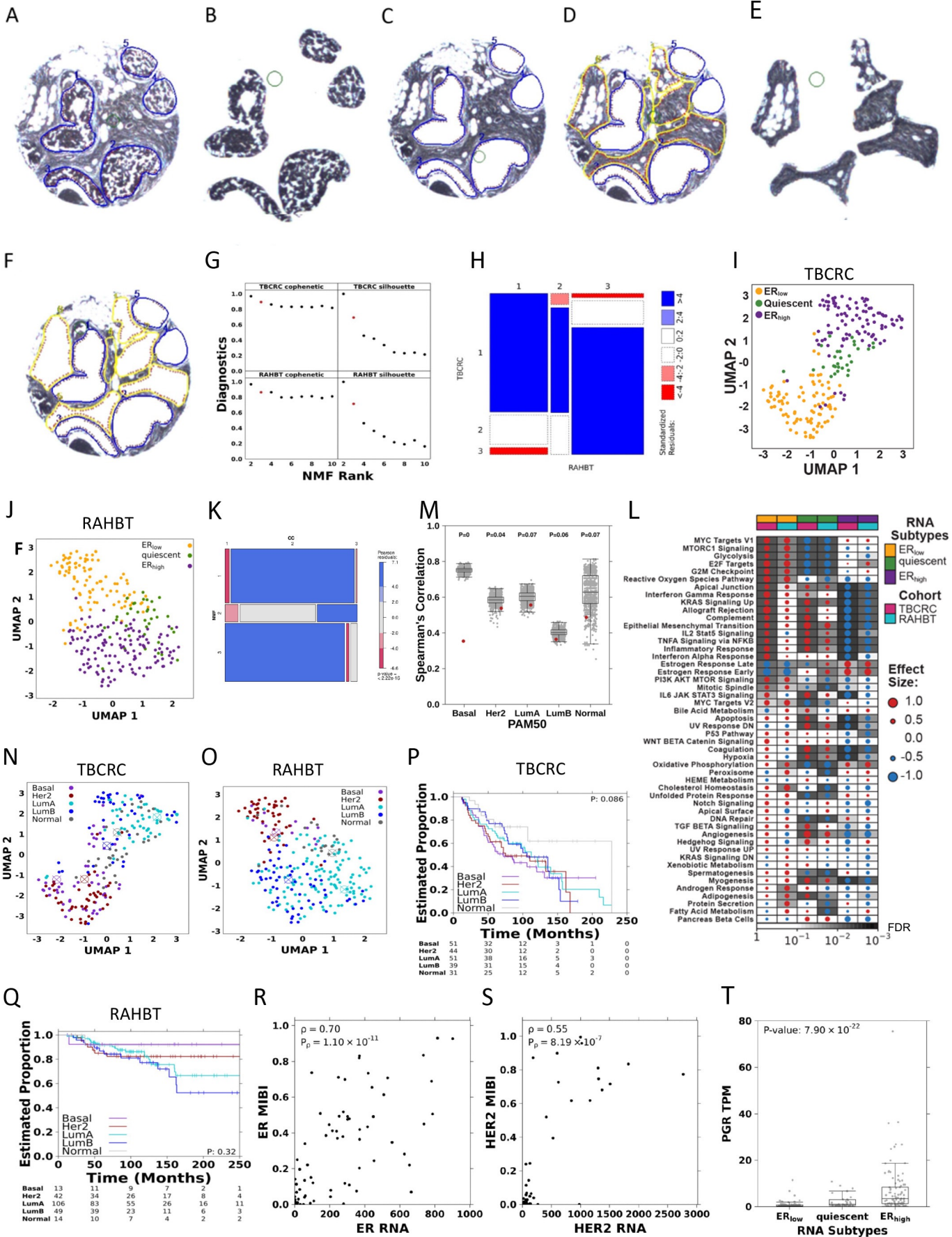


Figure S2: LCM dissection of RAHBT epithelial and stromal samples, and subtype characterization, related to Figure 4.

A) Marked DCIS epithelium (blue) prior to dissection. **B)** Dissected DCIS epithelium on cap. **C)** Remaining tissue on slide after dissection. **D)** Marked stroma (yellow) adjacent to dissected DCIS epithelium (blue, panel A-C) prior to dissection. **E)** Dissected stroma on cap. **F)** Remaining tissue on slide after dissection of DCIS epithelium and adjacent stroma. All images taken at 2X magnification. **G)** NMF diagnostic scatterplots show cophenetic and silhouette values with increasing numbers of clusters in TBCRC and RAHBT. **H)** Mosaic plot showing concordance of *de novo* clustering in RAHBT vs clusters determined from centroids identified in TBCRC. Blue indicates an enrichment while red indicates a depletion. **I-J)** UMAP projection of DCIS transcriptome colored by *de novo* RNA clusters in TBCRC (**I**) and RAHBT (**J**). **K)** Mosaic plot showing concordance between clusters obtained by NMF and consensus clustering (CC) of TBCRC cohort (85.6% concordance). **L)** GSEA Hallmark pathway analysis of each cluster vs rest for TBCRC and RAHBT LCM in full . Size of the dot and color represents the magnitude and direction of pathway deregulation, *i.e.*, blue indicates the pathway is downregulated while red indicates the pathway is upregulated. Background shading indicates FDR. Effect size and FDR from GSEA algorithm. **M)** Boxplot shows median Spearman ρ of DCIS and IBC samples with PAM50 centroids. IBC samples were randomly downsampled 1,000 times to match the DCIS cohort size. Grey dots present median Spearman ρ of downsampled cohort. The red dot represents the median Spearman ρ of the DCIS cohort. P-values were calculated as 1- the proportion of downsampled IBC cohorts with median Spearman ρ greater than the DCIS cohort. Boxplot represents median, 0.25 and 0.75 quantiles with whiskers at 1.5x interquartile range. **N-O)** UMAP projection of DCIS transcriptome in TBCRC (**N**) and RAHBT LCM (**O**) colored by PAM50 subtype. Large circles represent the PAM50 subtype centroids. **P-Q)** Kaplan-Meier plots of time to progression in PAM50 subtypes in TBCRC (**P**) and RAHBT (**Q**). P-values from log-rank test. **R-S)** Correlation between mRNA abundance and MIBI protein levels of *ESR1/ER* (**R**) and *ERBB2/HER2* (**S**). Correlations coefficients and P-values from Spearman's correlation. **T)** *PGR* mRNA abundance in the three DCIS subtypes. P-value from Kruskal-Wallis test. Boxplot represents median, 0.25 and 0.75 quantiles with whiskers at 1.5x interquartile range.

Table S4: Associations between recurrent CNAs and sequencing coverage or cohort. Related to Figure 5.

| Recurrent CNAs | Association with coverage | | | Association with cohort | | |
|----------------|---------------------------|----------|-------|-------------------------|---------|--------------|
| | Difference in medians | P-values | FDR | Difference in medians | P-value | FDR |
| Amp_1q42.3 | 1550611 | 0.321 | 0.416 | 0.033 | 0.757 | 0.955 |
| Del_17p13.2 | 2800768 | 0.931 | 0.931 | 0.058 | 0.444 | 0.804 |
| Amp_17q12 | 2800768 | 0.651 | 0.697 | 0.044 | 0.587 | 0.895 |
| Amp_17q23.2 | 1737324 | 0.758 | 0.784 | 0.044 | 0.954 | 0.996 |
| Del_16q24.1 | 1217342 | 0.349 | 0.431 | 0.222 | 0.102 | 0.591 |
| Amp_8q24.21 | 2532147 | 0.882 | 0.897 | -0.071 | 0.348 | 0.745 |
| Del_11q25 | -6290327 | 0.618 | 0.674 | -0.196 | 0.644 | 0.903 |
| Amp_8q13.1 | -8252690 | 0.139 | 0.206 | 0 | 0.654 | 0.903 |
| Amp_20q13.2 | 7046467 | 0.132 | 0.201 | 0 | 0.436 | 0.804 |
| Del_11q22.3 | 13158102 | 0.032 | 0.058 | 0 | 0.314 | 0.745 |
| Amp_17q21.31 | -2459037 | 0.180 | 0.259 | 0 | 0.996 | 0.996 |
| Amp_8p11.23 | 20778292 | 0.036 | 0.062 | 0 | 0.957 | 0.996 |
| Del_3p14.1 | 2684015 | 0.729 | 0.767 | 0 | 0.163 | 0.599 |
| Del_8p11.22 | 1648757 | 0.518 | 0.585 | 0 | 0.343 | 0.745 |
| Amp_11q13.3 | 13932379 | 0.423 | 0.486 | 0 | 0.757 | 0.955 |
| Del_17q12 | -8452507 | 0.353 | 0.431 | 0 | 0.575 | 0.895 |
| Del_17q21.2 | 10296570 | 0.207 | 0.281 | 0 | 0.993 | 0.996 |
| Amp_19q13.12 | 10494689 | 0.341 | 0.431 | 0 | 0.338 | 0.745 |
| Amp_12q15 | -12560166 | 0.050 | 0.081 | 0 | 0.029 | 0.233 |
| Del_11p15.4 | 3708923 | 0.304 | 0.403 | 0 | 0.275 | 0.745 |
| Del_5q31.1 | 8548178 | 0.388 | 0.455 | 0 | 0.827 | 0.996 |
| Del_11q11 | -166682 | 0.610 | 0.674 | 0 | 0.531 | 0.895 |
| Del_1p21.3 | 18621923 | 0.044 | 0.073 | 0 | 0.002 | 0.028 |
| Del_11q13.1 | 10494689 | 0.061 | 0.095 | 0 | 0.165 | 0.599 |
| Amp_16q12.2 | -7615355 | 0.367 | 0.439 | 0 | 0.032 | 0.233 |
| Del_4q35.2 | -11531034 | 0.200 | 0.277 | 0 | 0.157 | 0.599 |
| Amp_6q25.1 | -7615355 | 0.182 | 0.259 | 0 | 0.360 | 0.745 |
| Del_10p15.3 | -21959310 | 0.027 | 0.050 | 0 | 0.000 | 0.005 |
| Del_19p13.3 | -30105171 | 0.042 | 0.072 | 0 | 0.904 | 0.996 |

Figure S3

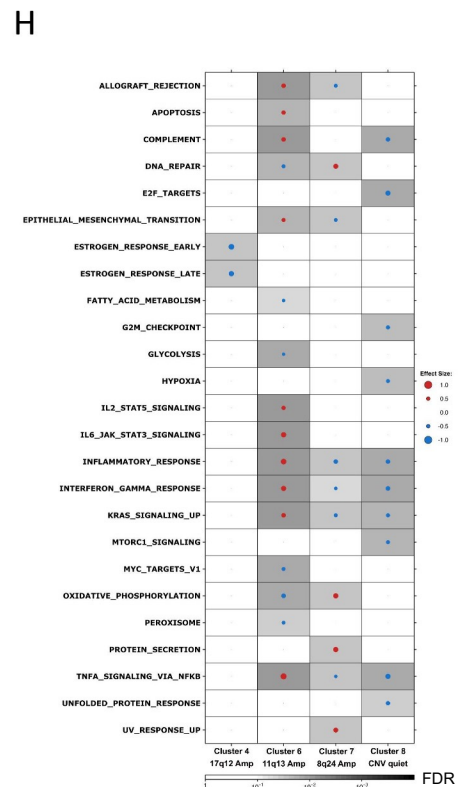
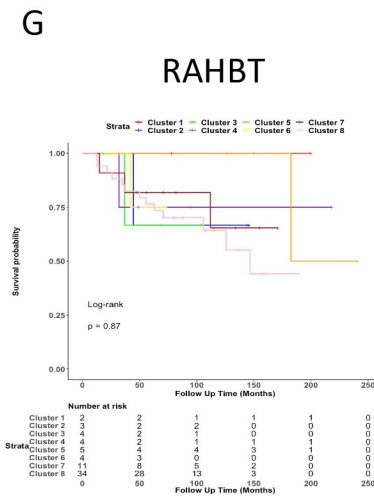
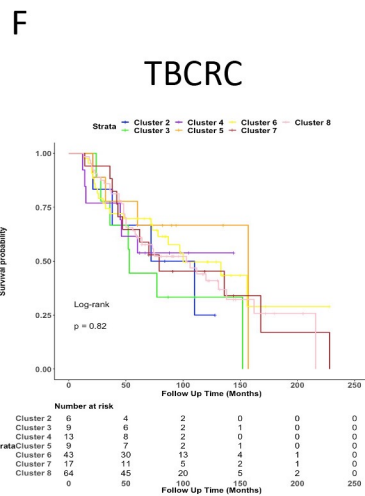
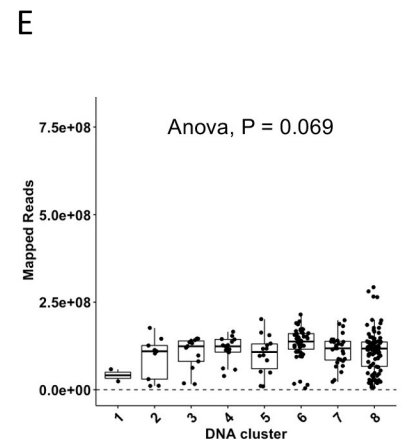
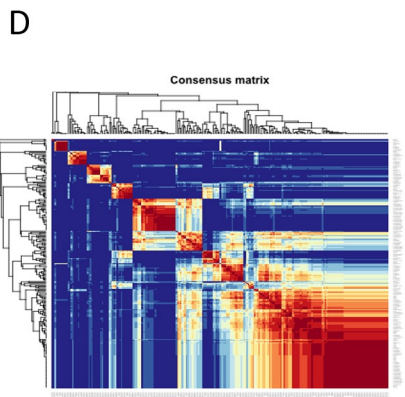
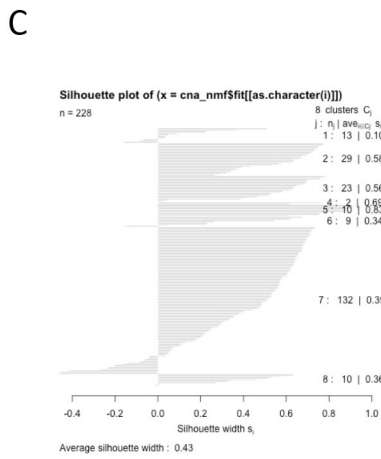
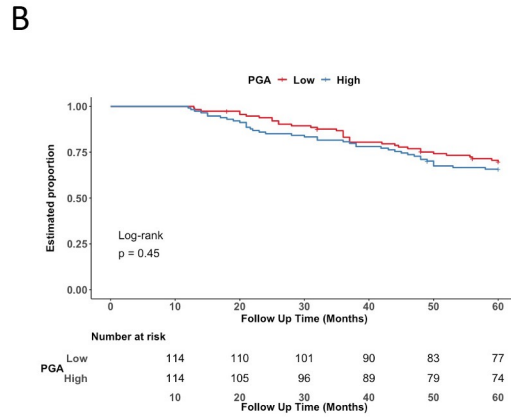
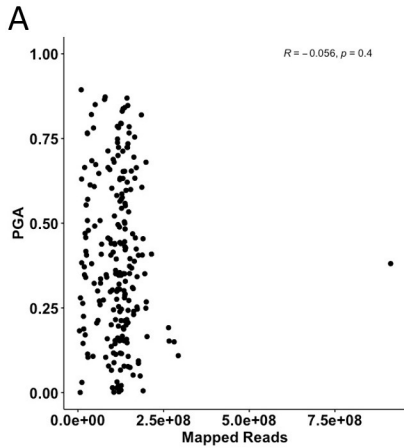


Figure S3: Characterizing the CNA landscape of DCIS, related to Figure 5.

A) Correlation between PGA and mapped reads. Correlation coefficient and P-value from Pearson Correlation. **B)** Kaplan-Meier plot of time to progression (any iBE, full follow-up) stratified by PGA (median dichotomized). P-value from log-rank test. **C)** Silhouette plot from NMF unsupervised clustering of the CNA landscape of DCIS in TBCRC and RAHBT combined. **D)** Consensus matrix from NMF unsupervised clustering of the CNA landscape of DCIS in TBCRC and RAHBT combined. **E)** Box plots of mapped reads in the eight DNA clusters. P-value from ANOVA. Boxplot represents median, 0.25 and 0.75 quantiles with whiskers at 1.5x interquartile range. **F-G)** Kaplan-Meier plot of time to progression stratified by the eight CNA clusters in TBCRC (**F**) and RAHBT (**G**). P-values from log-rank tests. **H)** GSEA Hallmark pathway analysis of DE genes by DNA cluster in matched RNA samples (each cluster vs rest) for TBCRC and RAHBT in full. Size of the dot and color represents the magnitude and direction of pathway deregulation, *i.e.*, blue indicates the pathway is downregulated while red indicates the pathway is upregulated. Background shading indicates FDR. Effect size and FDR from GSEA algorithm. Clusters with no significant pathway enrichment or depletion not included in plot.

Figure S4

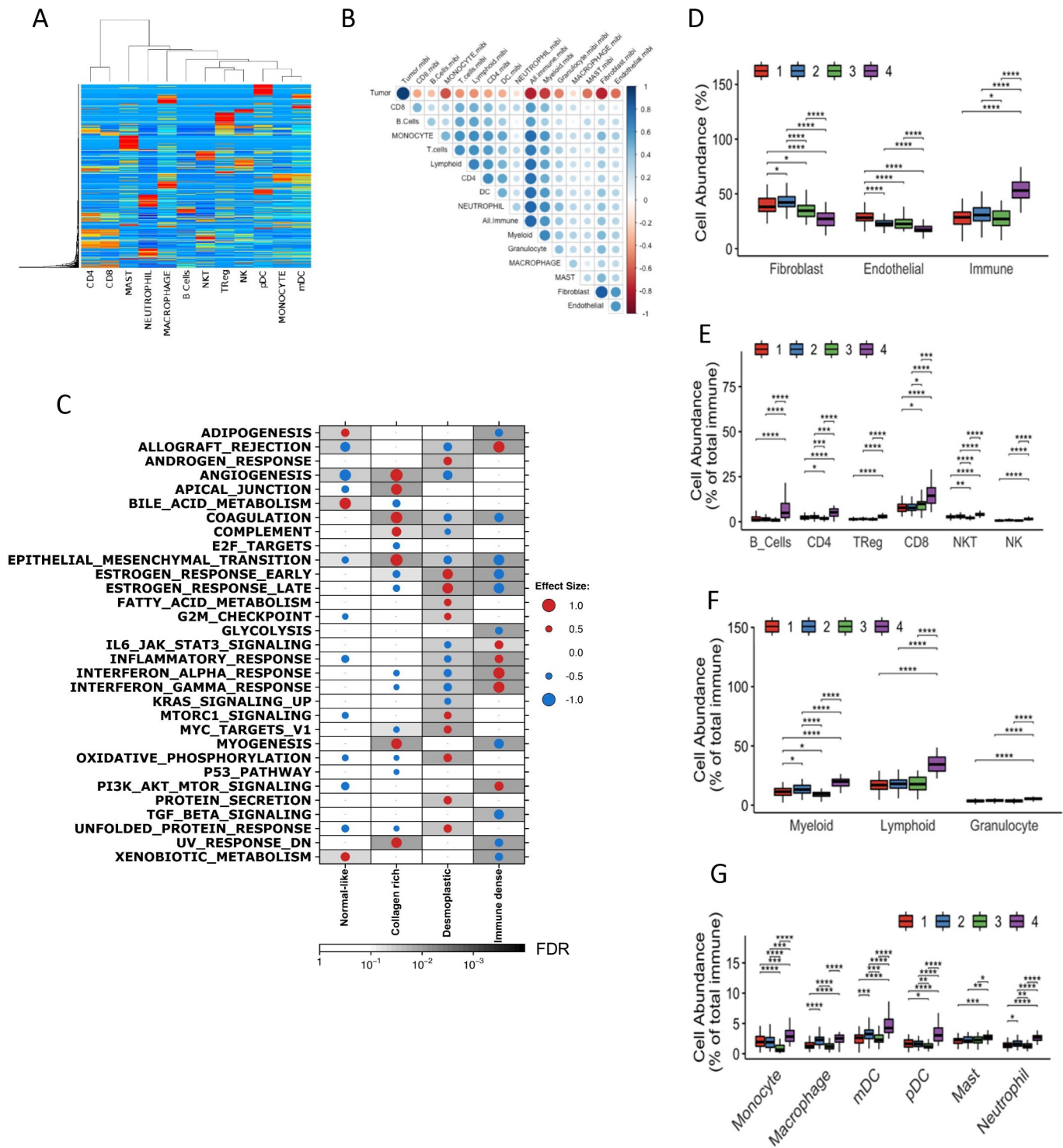
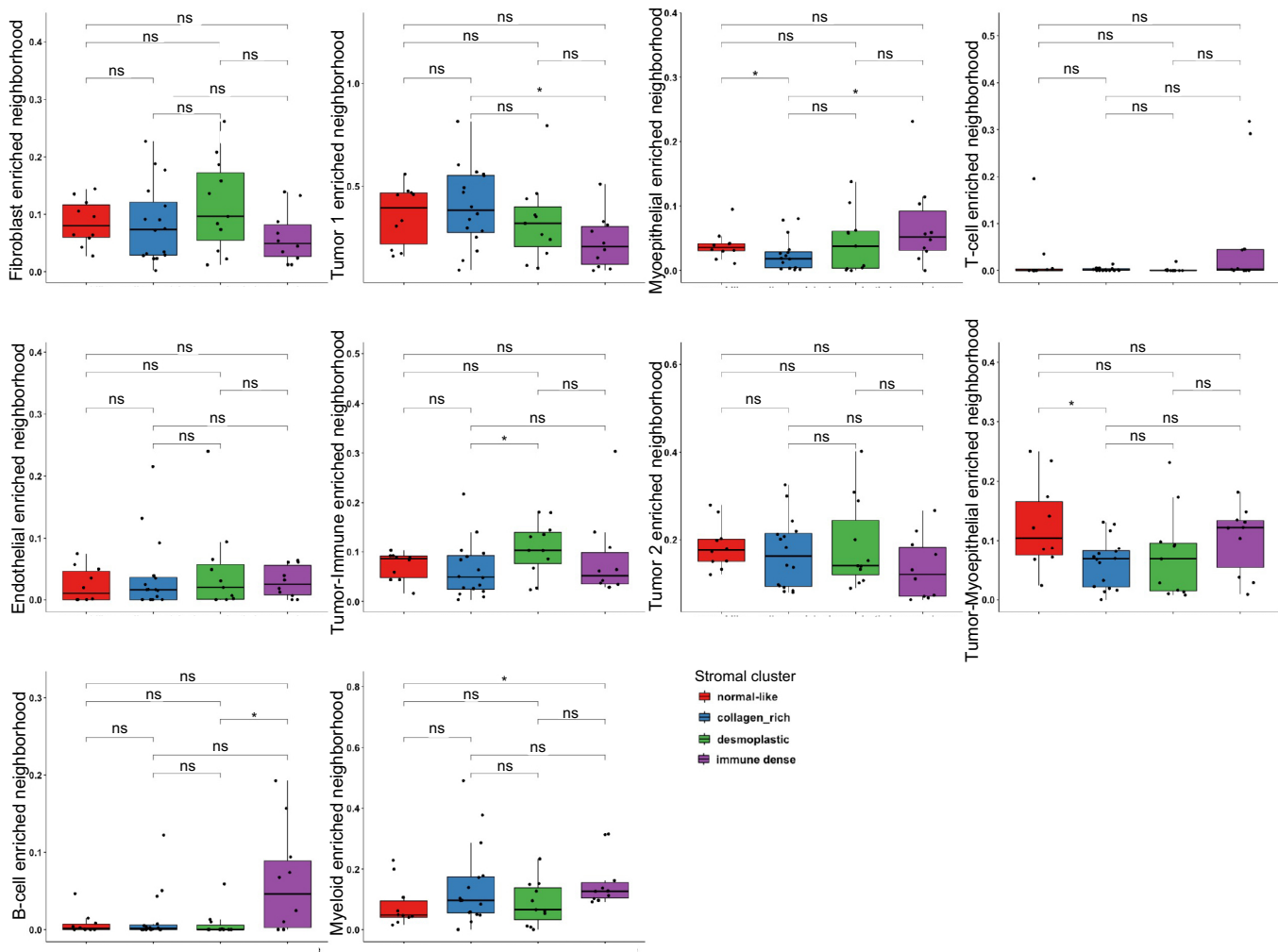


Figure S4: Analysis of the tumor microenvironment, related to Figure 6.

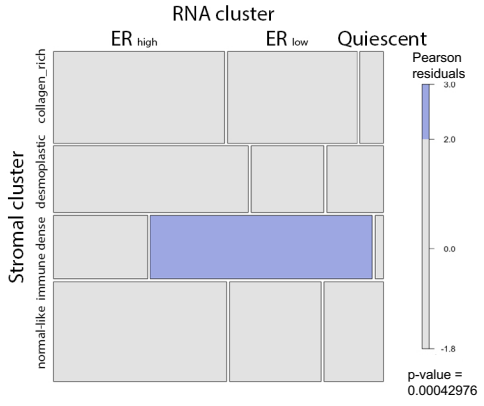
A) Heatmap showing signature matrix created using CibersortX (CSx) with 12 different immune cell types. **B)** Protein validation of CSx signature matrix by MIBI. Correlogram showing MIBI-based vs CSx-estimated cell types in RAHBT LCM samples. Correlation and statistics from Pearson's correlation. White background: $P > 0.05$. **C)** GSEA Hallmark pathway analysis of DE genes in each stromal cluster vs the rest in RAHBT LCM stromal samples in full. Size of the dot and color represents the magnitude and direction of pathway deregulation, *i.e.*, blue indicates the pathway is downregulated while red indicates the pathway is upregulated. Background shading indicates FDR. Effect size and FDR from GSEA algorithm. **D)** Percentage of fibroblasts, endothelial and total immune cells present in each stromal cluster estimated by CSx. **E)** Abundance of total myeloid, lymphoid and granulocyte cells, represented as percentage of total immune cells. **F-G)** Abundance of 12 immune cell types (percentage of total immune cells) by stromal clusters. Box plots (**D-G**): Red: Normal-like. Blue: Collage rich. Green: Desmoplastic. Purple: Immune dense. *: FDR < 0.05 ; **: FDR < 0.01 ; ***: FDR < 0.001 ; ****: FDR < 0.0001 ; ns: FDR > 0.05 (Wilcoxon rank sum test). Boxplots represent median, 0.25 and 0.75 quantiles with whiskers at 1.5x interquartile range.

Figure S5

A



B



C

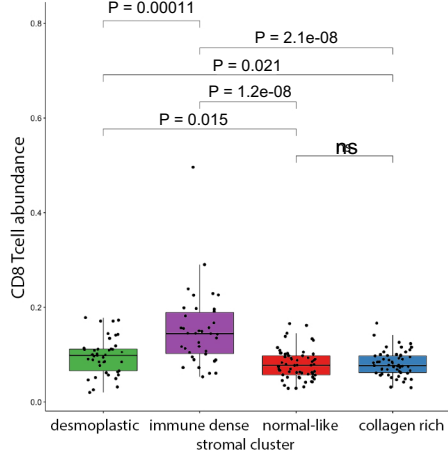
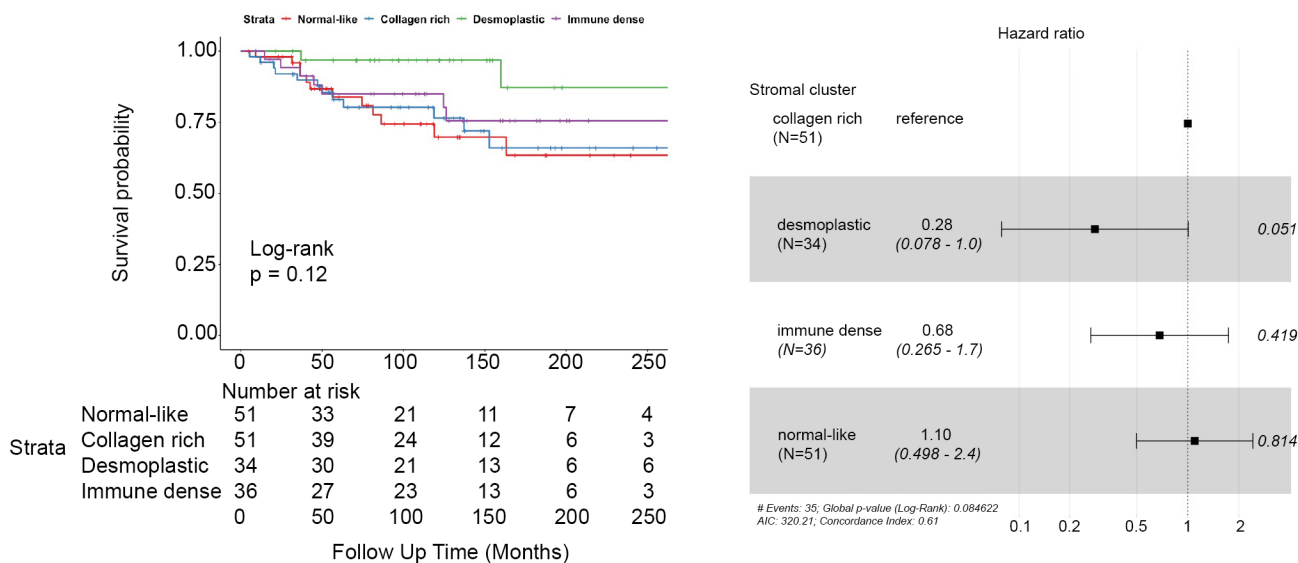


Figure S5: Analysis of the four stromal clusters using CSx and MIBI, related to Figure 6.

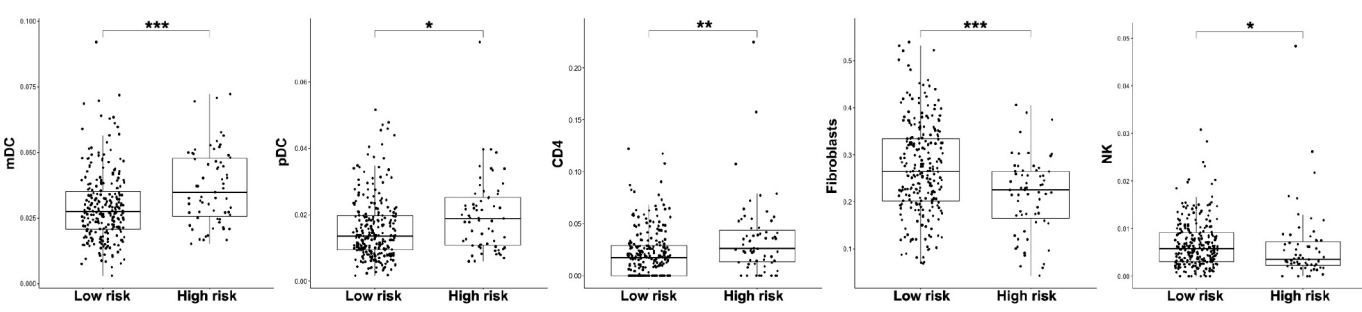
A) Cell neighborhood frequencies from MIBI by stromal clusters. *: FDR <0.05. ns: FDR >0.05 (Wilcoxon rank sum test). **B)** Mosaic plot showing correlation between the stromal clusters and the RNA 3-cluster subtypes in matched epithelial samples. **C)** Box plots showing the CD8 T-cell abundance by CSx in the four stromal clusters P-values from Wilcoxon rank sum test. **A, C):** Boxplots represent median, 0.25 and 0.75 quantiles with whiskers at 1.5x interquartile range.

Figure S6

A



B



C

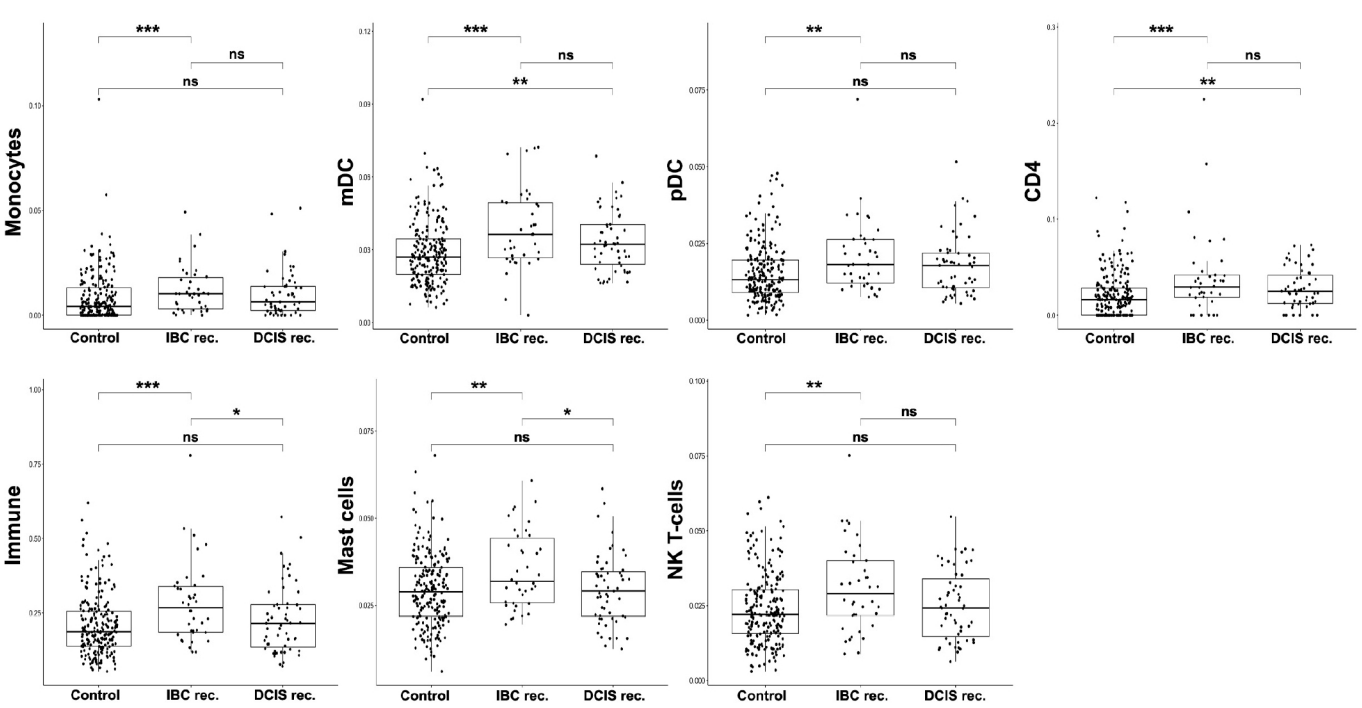


Figure S6: Outcome associations in the four stromal clusters, related to Figure 6.

A) Kaplan-Meier and forest plot of time to progression (any iBE, full follow-up time) stratified by stromal clusters in RAHBT LCM. Kaplan-Meier P-value from log-rank test. Forest plot P-values and hazard ratios from Cox multivariable analysis. **B)** CSx-inferred cell type distribution between 812 gene classifier risk groups (TBCRC and RAHBT combined). Only cell types with $FDR < 0.05$ are shown. **C)** CSx-inferred cell type distribution between cases with IBC iBEs, DCIS iBEs, and controls (TBCRC and RAHBT combined). Only cell types with $FDR < 0.05$ are shown. **B, C)** * $FDR < 0.05$. ** $FDR \leq 0.1$. *** $FDR \leq 0.001$; ns: $FDR > 0.05$ (Wilcoxon rank sum test). mDC: myeloid dendritic cells. pDC: plasmacytoid dendritic cells. NK: Natural killer cells. Boxplots represent median, 0.25 and 0.75 quantiles with whiskers at 1.5x interquartile range.

Table S5: Univariate Cox regression analysis of CSx cell type abundance towards progression (any iBE) in RAHBT LCM. Related to Figure 6.

| | coef | Exp (coef) | Se (coef) | z | P-value | FDR |
|-------------------|-------------|-------------------|------------------|------------|----------------|-------------------|
| mDC | 25.36863 | 1.041E+11 | 6.383095 | 3.974347 | 7.06E-05 | 0.00101071 |
| CD4 | 10.88261 | 53242.31 | 2.838826 | 3.833489 | 0.00012634 | 0.00101071 |
| pDC | 28.35189 | 2.06E+12 | 8.856115 | 3.201391 | 0.00136766 | 0.00554251 |
| Immune | 2.605316 | 13.5355 | 0.8147652 | 3.197628 | 0.00138563 | 0.00554251 |
| NKT | 19.62875 | 334702207 | 8.055231 | 2.436771 | 0.01481907 | 0.04595117 |
| Fibroblast | -2.624797 | 0.07245444 | 1.102057 | -2.381727 | 0.01723169 | 0.04595117 |
| Macrophage | 15.06461 | 3487218 | 6.808633 | 2.212576 | 0.02692691 | 0.06154722 |
| Mast | 19.44246 | 277813316 | 9.526299 | 2.040925 | 0.0412583 | 0.0825166 |
| Monocyte | 11.71033 | 121823.5 | 7.007859 | 1.671028 | 0.09471613 | 0.16838423 |
| Endothelial | -3.857939 | 0.02111147 | 2.48589 | -1.551935 | 0.1206778 | 0.19308448 |
| CD8 | 5.864071 | 352.1549 | 4.018355 | 1.459321 | 0.1444767 | 0.21014793 |
| Neutrophil | 20.47718 | 781856966 | 14.86406 | 1.377631 | 0.1683173 | 0.22442307 |
| T Reg | 11.2979 | 80651.73 | 10.19587 | 1.108086 | 0.2678248 | 0.32963052 |
| B Cells | 7.016958 | 1115.388 | 7.655518 | 0.9165882 | 0.3593585 | 0.41069543 |
| NK | 7.482623 | 1776.895 | 18.85228 | 0.396908 | 0.6914353 | 0.73753099 |
| Epithelial | -0.1520237 | 0.8589679 | 0.6357247 | -0.2391345 | 0.8110013 | 0.8110013 |

mDC: myeloid dendritic cells. pDC: plasmacytoid dendritic cells. NKT: Natural killer T cells.
 NK: Natural killer cells.